COMPARING THE WAVELET AND WAVELET PACKETS FEATURE SPACES IN MRSI BRAIN TUMOR CHARACTERIZATION

Azadeh Yazdan-Shahmorad, [1] *Hamid Soltanian-Zadeh,* [1, 2] *Reza A. Zoroofi*[1]

[1]Control and Intelligent Processing Center of Excellence, Electrical and Computer Engineering Department, Faculty of Engineering, University of Tehran, Tehran, Iran
[2]Image Analysis Lab., Radiology Department, Henry Ford Health System, Detroit, Michigan, USA

ABSTRACT

MRSI is an efficient approach to specify chemo-physical structures of living organs non-invasively. The need to differentiate between normal and abnormal tissues and determine type of abnormality before biopsy or surgery motivated development and application of MRSI. This paper compares wavelet and wavelet packets feature spaces in the analysis of MRSI using artificial neural networks. The purposed methods were applied to the brain spectra of patients with three tumor types (Astrocytoma, Oligodendroglioma and Malignant Glioma). The results of classifying wavelet packets feature space show about 10% improvement compared to the wavelet. This shows that wavelet packets features can describe the spectra and the effects of lesions on them better than the wavelet features.

1. INTRODUCTION

One of the recent and important applications of nuclear magnetic resonance technology is Magnetic Resonance Spectroscopic Imaging (MRSI) [1]. The major clinical applications of MRSI have focused on the examination of tissues for the purpose of diagnosis of disease or for the monitoring of therapeutic treatments non-invasively [2]. The MRSI measured from a tissue provides a wealth of information about the biochemicals contained within it [2]. Therefore considering the effects of the diseases on the tissue biochemicals, applying appropriate processing methods to MRSI data could extract useful information and improve the diagnosis. In recent years, a variety of investigations and research have been reported on the diagnostic applications of these signals [3]. Our final goal is to develop novel processing methods to determine the type of abnormality automatically. In this paper we compare two feature spaces using wavelets and wavelet packets extracted from brain MRSI data in differentiating between normal tissues and tumors and between three different brain tumor types.

2. MRSI BRAIN SPECTRA

As in imaging, there are technical reasons that make the brain easier than other organs to examine with MRSI: motion artifacts are minor, shimming is relatively easy to perform, and there is no detectible lipid in normal brain tissue [3]. Mobile lipids may appear as part of pathology such as necrosis tumors [4]. Another advantage of MRSI in the brain is that it does not require a special coil and may be incorporated at the end of a standard brain MRI [1]. In addition, due to non-invasive property of this method, it could be a good candidate for brain diagnostics.

Figure 1 shows typical MRSI spectra of the normal human brain from a clinical 1.5 T MR scanner. This spectrum is characterized by three major peaks called metabolits: creatine (Cr), choline (Cho), and N-Acetyl Asparatine (NAA) [2].

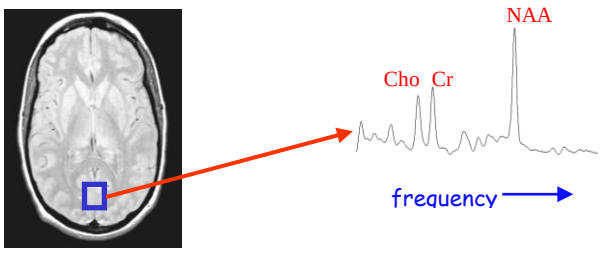

Figure 1. A real brain MRSI signal and the metabolite peaks creatine (Cr), choline (Cho), and N-Acetyl Asparatine (NAA).

Cr is involved in energy production in cell mitochondria [3]. Cr has been considered to be stable enough to be used as an internal reference in reporting relative concentrations of other brain metabolites, but recent findings suggest that this assumption should be used by care [5]. Cho takes part in membrane and neurotransmitter synthesis. Cho is thought of as a product of myelin breakdown [3]. NAA is the dominant peak in normal adult brain spectra. It is accepted as a neuronal and axonal marker whose physiological role is currently unknown [6]. Reduced NAA has been observed with

many neurological diseases that causes neuronal and axonal degenerations [3]. A diseased spectrum is shown in Figure 2.

It is also possible to observe some other peaks in brain spectra. For example, mobile lipid signals resulting from pathology appear as sharp peaks. They are seen in some tumors, stroke and acute MS lesions, and appear to be associated with acute destruction of myelin [7].

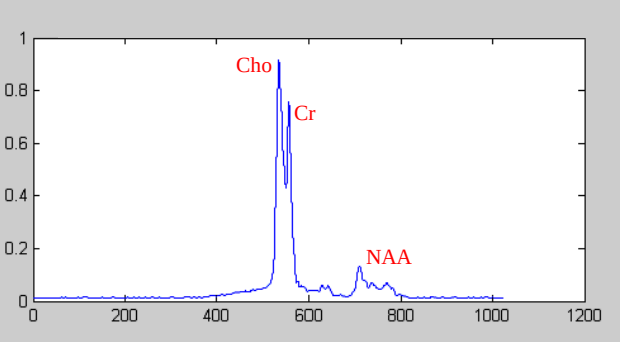

Figure 2. A diseased spectrum and the metabolite peaks creatine (Cr), choline (Cho), and N-Acetyl Asparatine (NAA) related to a patient with coagulation necrosis.

Interpretation of MRSI spectra consists of identification of the various spectral peaks, calculation of the relative or absolute metabolite concentrations and determination of peak shifts [3]. In many situations, qualitative data interpretation may quickly provide the needed answers [2]. However it is the ability to assess metabolite levels that gives the MRSI a clear advantage over other clinical imaging techniques. Accurate and reliable quantification, when achieved and routinely applied, will have the biggest impact on the clinical utility of MRSI. In most clinical situations, some type of quantification is essential for assessing metabolite levels in patients compared to those in healthy individuals, and for monitoring changes in metabolite levels of patients undergoing treatment [7]. A major factor in the acceptance of in vivo MRSI as a useful clinical tool relies on its ability to provide an accurate and reproducible means for determining metabolite levels [1].

Our goal in this research was to detect and segment tissue abnormalities by extracting the biochemical features related to these peaks in the MRSI data of brains with tumors. Each of these metabolites has a specific role in the brain tissue and based on available clinical data, each brain lesion will have different effects on these metabolites [8].

3. METHODS

Analysis of this signal may be performed in different ways, but the goals of any analytic method are the following: presentation of MRSI data in an easily interpretable format, assignment of measured signals to specific metabolites, and robust determination of the relative or absolute metabolite concentrations [9]. We applied different processing methods in order to extract useful feature spaces from the spectrum.

3.1. Wavelet feature space

The first step in any MRSI data evaluation is identification of the various spectral peaks and their assignments to particular metabolites [3]. Complete peak identification requires determination of peak positions and characteristics [5]. Peak identification alone may be useful in instances where only verification of the presence or absence of a given metabolite is needed. For example, in the brain spectra an obviously absent NAA peak helps confirm suspicion of damage or loss of neurons or axons [10].

We use wavelet transform (Daubechie10) for analyzing the local areas related to each peak and segregate metabolite peaks by thresholding the wavelet coefficients and finally reconstruct a signal from the remaining coefficients. The threshold value depends on MR scanner and patient conditions. Our approach calculates it automatically using the mean value of the wavelet coefficients. This signal contains the peaks without minor details that prevent automatic estimation of the peaks locations. We estimate the peaks locations from this signal. Then, we calculate the peaks features using the original signal that contains all the information.

The use of MRSI for quantitative analysis depends on the fact that, if certain conditions are met, the area under a peak is directly proportional to the number of spins contributing to the peak [3]. Therefore, under appropriate conditions in MRSI evaluation, assessment of metabolite relative or absolute concentrations can be reduced to calculation of peak areas, also referred to as peak integrals [3]. In order to have a complete feature space we extracted peak height, peak bandwidth, and the mean value of wavelet coefficients in the peak region rather than peak area. Peak area calculation by itself is not sufficient for accurate assessment of concentrations [11]. An easy assessment of variations in metabolite levels consists of evaluating metabolite peak area ratios [3, 11]. Therefore, we calculated the peak area ratios and added them to the wavelet feature space. The disadvantage of using ratios is that changes in either or both metabolite concentrations affect the ratio.

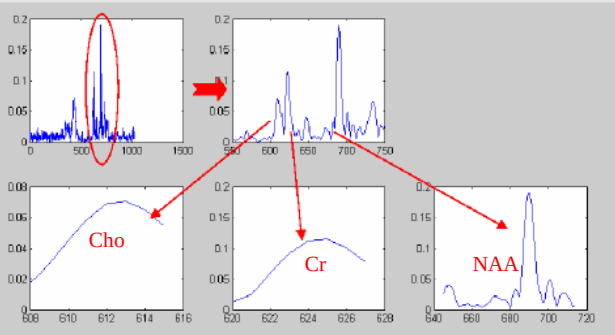

Figure 3. A normal brain MRSI signal and the separated metabolite peaks creatine (Cr), choline (Cho), and N-Acetyl Asparatine (NAA) using wavelet transform.

3.2. Wavelet packets feature space

The wavelet packet method is a generalization of wavelet decomposition that offers a richer range of possibilities for signal analysis [12]. In wavelet analysis, a signal is split into an approximation and a detail. The approximation is then split into a second-level approximation and detail, and the process is repeated [13]. In wavelet packet analysis, the details as well as the approximations can be split [12]. This offers the richest analysis, we applied the wavelet packets transform to the whole signal to analyze the signal rather than only the metabolite peaks. We applied wavelet packets algorithm to our signal for 3 levels (Daubechie10) and extracted the statistical parameters such as mean, maximum, and variance values of the coefficients of each sub-band. We used these statistical parameters as other features extracted from the signal. The Daubechie10 mother wavelet and level 3 were chosen from reference [12]. In this way, we had features expressing the whole signal characteristics despite the above method, in which we only used the features related to specific regions of the signal.

3.3. Artificial Neural Networks Classifiers

Neural network analysis of MRSI data has been successfully used for automatic classification of human brain tumors even though there were no statistically significant metabolite concentration differences between the tissue groups [14]. Results to date indicate that neural networks may distinguish among spectra whose differences are not apparent to the human observer [15].

We used multilayer perceptron neural networks to classify the features extracted from the spectra. We selected the number of neurons in the hidden layer by trial and error in 95% learning. The networks were trained to classify the spectra into two classes: normal and diseased. Additional classification of the different groups of patients, as defined from clinical data, was also performed. In this case, classification was attempted in two steps. In the first step we had three classes: normal, necrosis and tumor. The next step was to classify the tumor spectrums into three classes: Astrocytoma, Oligodendroglioma and Malignant Glioma. Data were divided into training, test, and verification groups. The first two groups were used for network architecture development and the latter was used as an additional independent measure of prediction accuracy. We used two feature spaces extracted from the spectra using wavelet transform and wavelet packets.

3.4. MRSI data

We used clinical and simulated MRSI data to evaluate the purposed processing methods and the extracted feature spaces.

The clinical data were the MRSI and biopsy results from the brains of patients (mean age = 43, range = 38-50, 28% female, 72% male) affected by three types of tumors (Astrocytoma, Oligodendroglioma, Malignant Glioma,) and focal necrosis. The MRSI data were acquired using a 1.5 T MRI System (GE Signa).

To generate the simulated MRSI data, we constructed three main peaks for the brain metabolites using Gaussian functions. We compiled these peaks with random width, amplitude, and location, and with a background signal. To create the background signal, we used appropriate number of Gaussian functions with appropriate width, location, and amplitude. Finally, we added white Gaussian noise to the inverse Fourier transform of the spectra and reconstructed the results into the simulations. We also used the available clinical data and the effect of each brain lesion on the spectra to simulate the spectra related to each lesion.

4. EXPERIMENTAL RESULTS

As discussed before, we classified the available data in three steps. In the first step we trained the network to classify the data into two classes: normal and diseased.

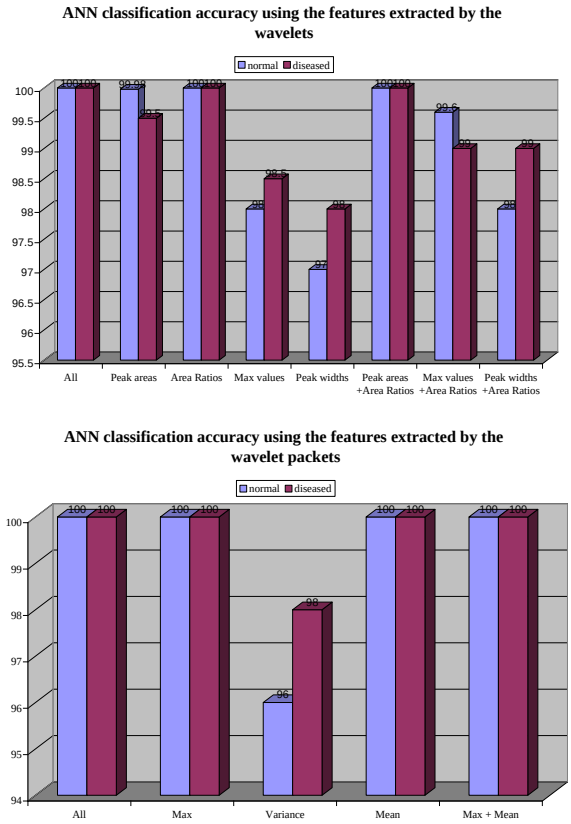

Figure 4. ANN classification into two classes: normal and diseased using the two feature spaces.

The results of this step are shown in the charts of Figure 4. In this step, in some cases we had 100 percent accuracy in classifying but if we compare the whole charts of the two feature spaces we find better results from wavelet packets feature space.

The results of classifying the extracted features into three classes (tumor, necrosis, and normal) for both of the methods are shown in the charts of Figure 5. We used different sets of the features for training and testing of the networks to find the best features. In the case of wavelet features (which are peak features) we obtained the best accuracy when we used peak area ratios, which was 90% for the test data. We also used different sets of wavelet packets features separately to find the best features in this domain. The results show about 7% improvement compared to the previous features. This shows that these features can describe the spectra and the effects of lesions on them better than the previous ones. In other words, this shows that each brain lesion has significant effects on the whole signal in addition to the metabolite peaks.

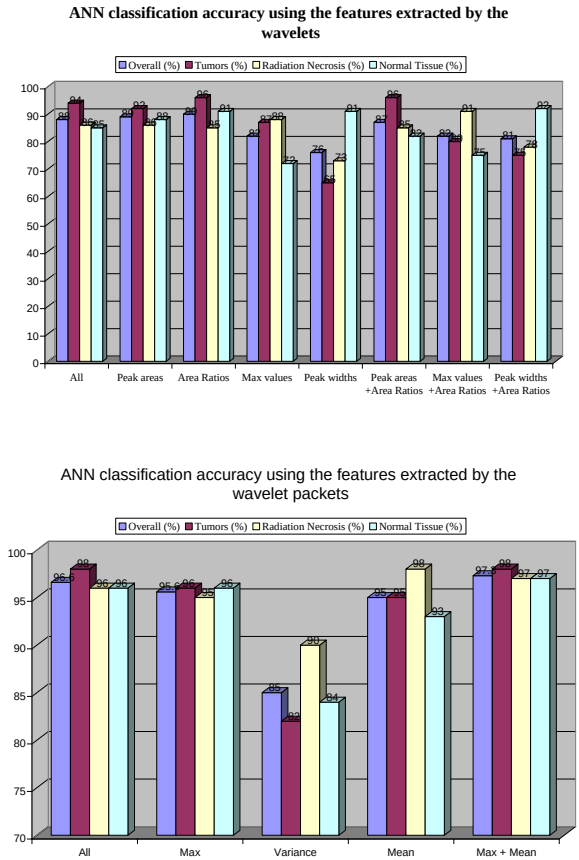

Figure 5. ANN classification into three classes: normal, radiation necrosis and tumor.

In the next step, we used artificial neural networks to classify the tumor spectra into 3 types (Glioma, Oligodendroglioma, and Astrocytoma). Due to the sample size limitation, we used a leave one out method for training and testing of the network. We used the same features in the previous methods. The best classification results were: 71% for Glioma, 75% for Oligodendroglioma and 69% for Astrocytoma. We also used the simulated spectra for each brain tumor type for training and testing of the network. The best classification results in this case were: 82% for Glioma, 85% for Oligodendro-glioma, and 83% for Astrocytoma.

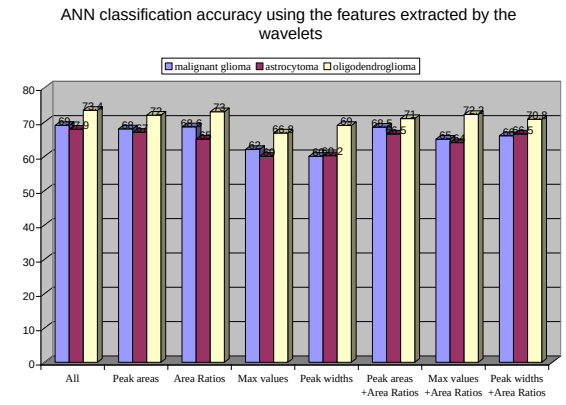

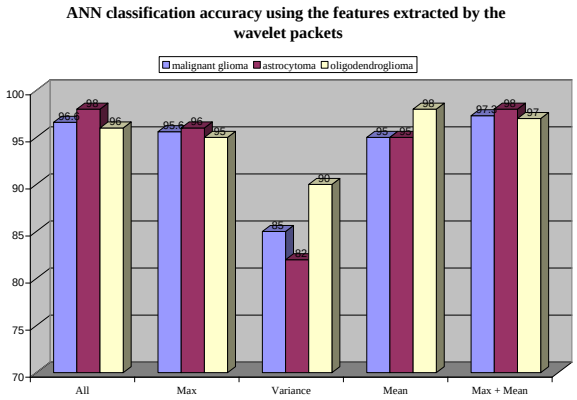

Figure 6. ANN classification into three classes: malignant glioma, astrocytoma and oligodendroglioma.

5. DISCUSSION

Although some network architectures could be designed to yield 100% correct predictions, it was relatively difficult to find a systematic series of parameters that yielded consistently acceptable predictive results. It was necessary to optimize (reduce) the total number of inputs in order to improve the prediction accuracy. For these reasons, the following approach, which was more consistently successful, was used.

The average true positive fraction, true negative fraction, false positive fraction, and false negative fraction for every different set were used [15]. It is one of the strengths of this approach that features considered to be too different from any used in the training set are not necessarily forced to be classified.

Comparing the average true positive fraction, true negative fraction, false positive fraction, and false negative fraction for every different set in the wavelet and wavelet packets feature spaces shows that the best sets in the wavelet feature space are the peak areas and area ratios. The accuracies of the networks trained with these features were 89% and 90%, respectively.

The best features in wavelet packets group, as seen in Figure 5, were the maximum and mean values of the coefficients of each sub-band of wavelet packets in level 3. The accuracies of the networks trained with these features were 95.6% and 95% for the maximum and mean, respectively. When we used both of these features for training the network, we obtained a higher accuracy at 97.3%.

We also applied this procedure to classify the tumors. In this case the best results were obtained from the same sets as before for both of the feature spaces. The fact is that in this step, as shown in the charts of Figure 6, the differences between the classification accuracies were less than the previous cases.

As discussed above, we selected the number of neurons in the hidden layer by trial and error in 95% learning. The network structures used for the classifications in each step are listed in Tables 1, 2.

Table 1. The feature sets extracted from the spectra using wavelet transform and the network structures for the three groups of classifying. The first one: classifying into two classes (normal and diseased), The second one: classifying into three classes (normal, necrosis and tumor), The third one: classifying into three classes (glioma, astrocytoma and oligodendroglioma).

Features	No. of Features	Network Structure for the first group	Network Structure for the second group	Network Structure for the third group
All	15	15-12-2	15-20-3	15-20-3
Peak areas	3	3-5-2	3-5-3	3-5-3
Area Ratios	6	6-5-2	6-5-3	6-5-3
Max values	3	3-7-2	3-7-3	3-7-3
Peak widths	3	3-7-2	3-7-3	3-7-3
Peak areas +Area Ratios	9	9-10-2	9-12-3	9-12-3
Max values +Area Ratios	9	9-10-2	9-12-3	9-12-3
Peak widths +Area Ratios	9	9-10-2	9-12-3	9-12-3

Table 2. The feature sets extracted from the spectra using wavelet packets and the network structures for the three groups of classifying. The first one: classifying into two classes (normal and diseased), The second one: classifying into three classes (normal, necrosis and tumor), The third one: classifying into three classes (glioma, astrocytoma and oligodendroglioma).

Features	No. of Features	Network Structure for the first group	Network Structure for the second group	Network Structure for the third group
All	24	24-10-2	24-12-3	24-12-3
Max	8	8-10-2	8-10-3	8-10-3
Variance	8	8-10-2	8-10-3	8-10-3
Mean	8	8-10-2	8-10-3	8-10-3
Max + Mean	16	16-12-3	16-10-3	16-10-3

6. CONCLUSION

MRSI is a non-invasive technique that allows direct observation of cerebral metabolites, including N-acetyl aspartate (NAA), creatine (Cr), and choline (Cho). We applied two processing methods using wavelets and wavelet packets to the MRSI spectrums to characterize brain tumors for clinical diagnosis. The results of classifying wavelet packets features show about 10% improvement compared to the wavelet features. This shows that these features can describe the spectra and the effects of lesions on them better than the previous ones. This also suggests that brain lesions affect the entire signal in addition to the metabolite peaks. We used different sets of the features for training and testing the networks to find the best features. In the case of wavelet features (which are peak features) we obtained the best

accuracy when we used peak area ratios, which was 90% for the test data. We also used different sets of wavelet packets features separately to find the best features in this domain. The best features in this group were the maximum and mean values of the coefficients of each sub-band of wavelet packets in level 3. The accuracies of the networks trained with these features were 95.6% and 95% for the maximum and mean, respectively. When we used both of these features for training the network, we obtained a higher accuracy at 97.3%. The results obtained in this research show about 4% improvement compared to the previous work [15].

7. REFERENCES

[1] D.D. Stark and W.G. Bradley, "*Magnetic Resonance Imaging*," Vol. 1,2nd Ed., Mosbey-yearbook, 1992.

[2] N. Salibi and M.A. Brown, "*Clinical MR Spectroscopy: First Principals*," 1998.

[3] I. Gerothanassis, A. Troganis, V. Exartue and K. Barbarrasoo, "Nuclear Magnetic Resonance (NMR) Spectroscopy: Basic Principles and Phenomena, and their Applications to Chemistry, Biology and Medicine,"*Chemistry Education: Research and Practice in Europe*, Vol. 3, No. 2, pp. 229-252, 2002.

[4] M. Tosi, R. Ricci, G. Bottura and V. Tugnoli, "In Vivo and In Vitro Nuclear Magnetic Resonance Spectroscopy Investigation of an Intracranial Mass," *Oncology Reports*, vol.8, pp.1337-1339, 2001.

[5] A. Horska, A. Ulug¡, E. Melhem, C. Filippi, P. Burger, M. Edgar, M. Souweidane, B. Carson and P. Barker, "Proton Magnetic Resonance Spectroscopy of Choroid Plexus Tumors in Children," *Journal of Magnetic Resonance Imaging*, vol.14, pp.78-82, 2001.

[6] W. Ende, D. F. Braus, P. Soher, F. Henn and C. Buchel, "A Fully Automated Method for Tissue Segmentation and CSF-Correction of Proton MRSI Metabolites Corroborates Abnormal Hippocampal NAA in Schizophrenia," *NeuroImage,* vol.16, pp.49–60, 2002.

[7] D. Wiedermanna, N. Schuffa, G. Matsonb, B. Sohera, A. Dua, A. Maudsleya and M. Weinera, " Short Echo Time Multislice Proton Magnetic Resonance Spectroscopic Imaging in Human Brain: Metabolite Distributions and Reliability," *Magnetic Resonance Imaging*, vol.19, pp.1073–1080, 2001

[8] M.R. Tosi, G. Fini, A. Tinti, A. Regiani and V. Tugnoli, "Molecular Characterization of Human Healthy and Neoplastic Cerebral and Renal Tissues by In Vitro 1H NMR Spectroscopy (Review)," *International Journal of Molecular Medicine*, vol.9, pp.299-310, 2002.

[9] S. Bonavita, F. Salle and G. Tedeschi, "Proton MRS in Neurological Disorders," *European Journal of Radiology*, vol.30, pp.125-131, 1999.

[10] S. Barton, F. Howe, A. Tomlins, S. Cudlip, J. Nicholson, B. Bell and J. Griffiths, "Comparison of In Vivo ^{1}H MRS of Human Brain Tumors with ^{1}H HR-MAS Spectroscopy of Intact Biopsy Samples In Vitro," *Magnetic Resonance Materials in Physics, Biology and Medicine*, vol.8, pp.121-128, 1999.

[11] P. Zamani and H. Soltanian-Zadeh, "Tissue Characterization by Fuzzy Clustering of Wavelet Denoised MRSI Data," *BioMed 2002 conference proceeding*, pp.9-11, 2002.

[12] L. Maindardi, D. Origgi, P. Lucia, A. Paganini, G. Scotti and S. Cerutti, "Automatic Extraction of H Magnetic Resonance Spectroscopy Parameters Using a Signal Decomposition Method Based Upon Wavelet Packets," *Proceedings- 19th International Conference- IEEE/EMBS Chicago, IL, USA* Oct.30- Nov.2, 1997.

[13] Akay M, *Time Frequency and Wavelets in Biomedical Signal Processing*, IEEE Press, New York, 1998.

[14] P. Lisboa, N. Branston, W. Deredy and A. Vellido, "Tissue Characterization with NMR Spectroscopy: Current State and Future Prospects for the Application of Neural Network Analysis," *International Conference on Neural Networks*, vol.3, 9-12 Jun, 1997.

[15] D. Axelson, I. Bakken, I. Gribbestad, B. Ehrnholm, G. Nilsen and J. Aasly, "Applications of Neural Network Analyses to In Vivo 1H Magnetic Resonance Spectroscopy of Parkinson Disease Patients," *Journal of Magnetic Resonance Imaging*, vol.16, pp.13–20, 2002.